Asad, Mohammad, Zahra, Tatheer, Thambiratnam, David P., Chan, Tommy H.T., Liu, Xuemei, Zhuge, Yan, Hayne, Mark, Morris, Anthony, & Nguyen, Christina
(2022)
Innovative impact testing machine for enhancing impact related research in Australia.
International Journal of Protective Structures, *13*(2), pp. 273-294.

https://doi.org/10.1177/20414196211073502

Innovative Impact Testing Machine for Enhancing Impact Related Research in Australia

Mohammad Asad[1]*, Tatheer Zahra[1], David P Thambiratnam[1], Tommy H.T. Chan[1], Xuemei Liu[2], Yan Zhuge[3], Mark Hayne[1], Anthony Morris[1], Christina Nguyen[1]

[1]Queensland University of Technology (QUT), Brisbane, QLD 4001, Australia.

[2]The University of Melbourne, Victoria 3010, Australia

[3]University of South Australia (UniSA), Adelaide 5001, Australia.

.

Abstract

This paper summarises the development of a state-of-art impact testing machine for simulating impacts such as vehicular crashes or debris impacts onto structures. The machine has a 200 kg pneumatically powered projectile which can travel horizontally within the barrel of the machine with a maximum velocity of 50 m/sec to impact the target structure. The maximum kinetic energy that can be generated by the projectile is 125 kJ by using different combinations of mass and velocity. The diameter of the projectile is 214 mm, and its impacting face can be changed to different shapes, such as flat circle, flat square or an elliptical nose to suit different impact scenarios. An innovative braking mechanism incorporating a crush tube is attached within the barrel to ensure safety when the projectile fails to be restrained by the impact. The crush tube can absorb the maximum imparted by the moving projectile. An advanced data acquisition system is installed to collect quantitative and qualitative test data during a period of 50ms to 1 sec. Two high-speed digital image correlation (DIC) cameras are attached and synchronised with the operation of the impact testing machine to record the images at the rate of 50,000 frames per second. Outputs in terms of strains, deformations, accelerations of the target structure with a record of damage history can be analysed using this 3D DIC technique. The paper also briefly presents the first application of this machine for impact testing masonry wall structures.

Keywords

Impact testing machine, vehicular crashes, pneumatic, projectile, strains, deformations, accelerations.

* Corresponding Author: Postdoctoral Research Fellow of Civil & Environmental Engineering, Gardens Point Campus, QUT, Brisbane, QLD 4001, Australia;
email: m.asad@qut.edu.au

1. Introduction

The number of human-induced disasters in modern cities is increasing exponentially due to deliberate and accidental events caused by population increases, industrialisation and the emergence of new technologies such as high-speed cars and nuclear power [1]. Critical infrastructure such as bridges, power plants and buildings are vulnerable to impacts, and terrorist attacks [2] and such incidents can cost billions of dollars for replacements, repairs, temporary relocations, clean ups, etc.[3]. According to the Swiss Re Institute report [4], human-induced hazards resulted in 3000 deaths in 118 events worldwide, resulting in economic losses of USD 7 billion in total in 2017 alone. From media reports and statistics on reported incidents, there are approximately 2000 vehicular crashes into roadside buildings per year causing considerable harm to occupants of buildings and vehicles as well as loss of property and disruption to lives. It is therefore important to understand the behaviour of vulnerable structural elements under impact loading to develop mitigation strategies and minimise the adverse consequences of such crashes.

There has been some research on developing safety measures for structures against impact through simplified experimental testing. Felice & Giannini [5], Freidenberg et al. [6], Gilbert et al. [7] and Mauro et al. [8] performed experiments to understand the global failure of building walls under different intensities of impact loadings. A broad investigation was carried out to categorise the range of detrimental impact velocities from low to high [9]. Asad et al. [10, 11] defined low velocity impact as an event where the contact time between the target and the impactor is relatively long, allowing time for the global response of the impacted body. Experimental testing machines which can simulate low velocity impact events are the drop weight impact testing machine [12-15], pendulum impact [16-19] and horizontal impact testing machine with drop weight mechanism [7] as shown in **Figure 1**. These machines can create global cracks on the surface of the structure or inflict minor damage depending on the type of structure and materials used [20]. High-velocity impact on the other hand, can be defined as an event where the impactor produces prominent localised damage in the target or enabled the penetration of the impactor through the impacted body [11, 21].

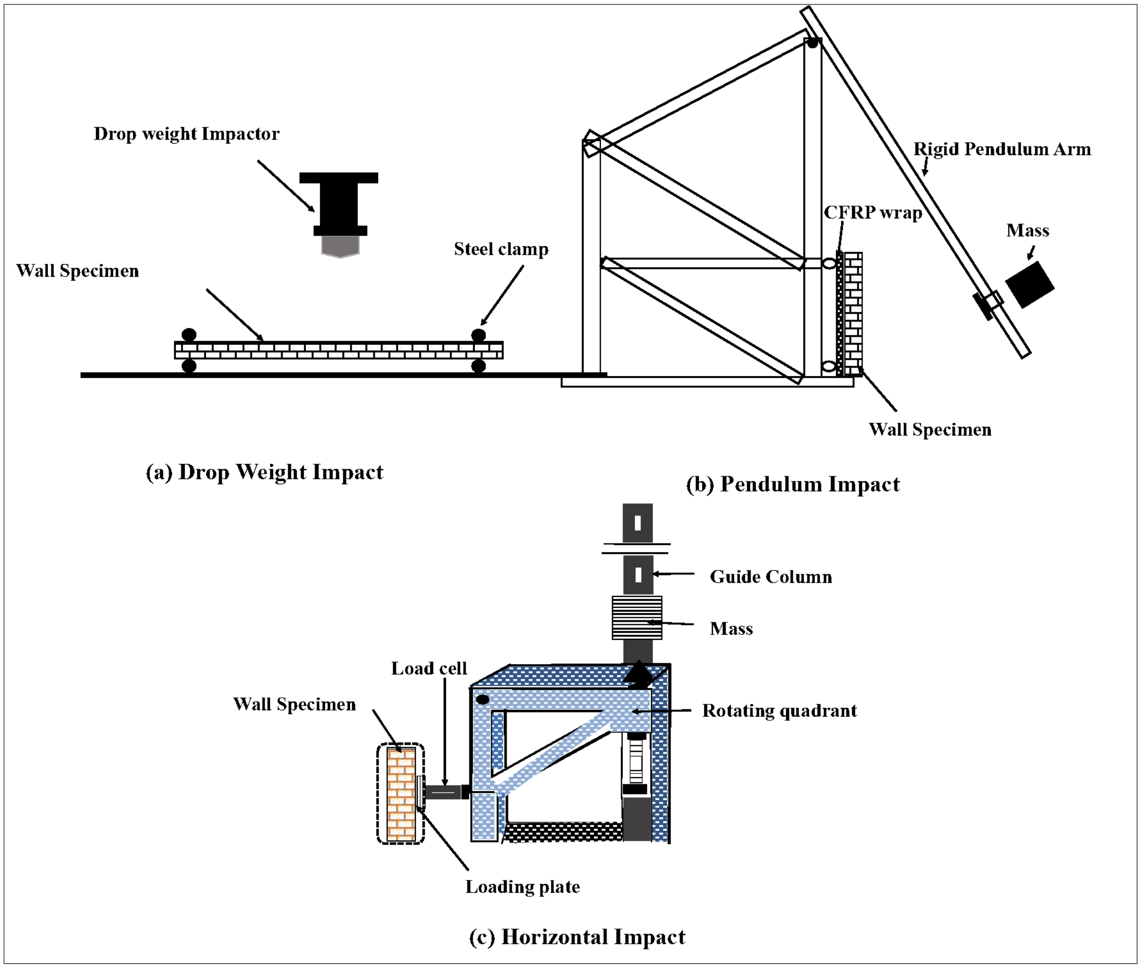

58

59 **Figure 1: Impact testing machines: (a) Drop Weight [22] (b) Swinging Pendulum [16] and (c)**
60 **Horizontal Impactor** [7]

61 The testing equipment developed for simulating high speed impacts is the tornado-generated
62 missile impact machine, as shown in **Figure 2**. A series of experimental tests have been
63 conducted using the tornado-generated missile impact machine in the laboratory [23-26].

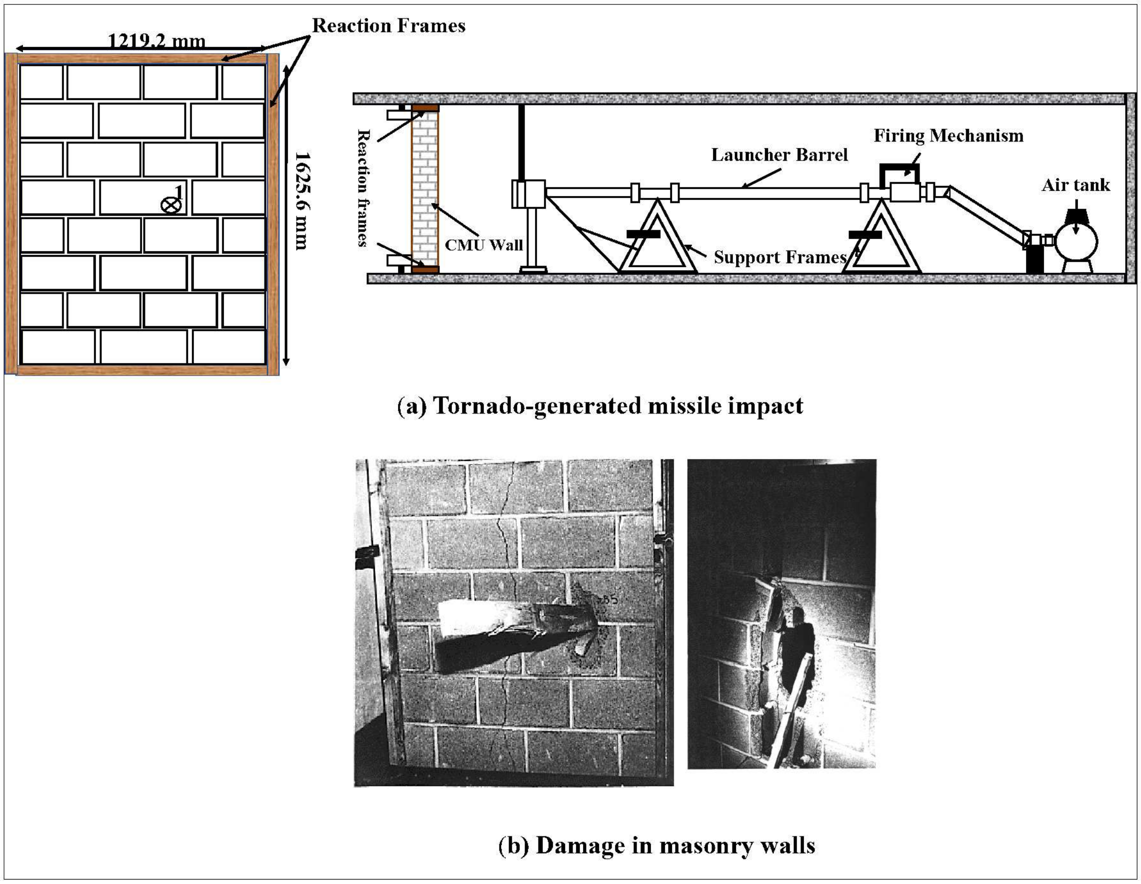

Figure 2: Experimental setup of wall and tornado generated missile impactor launcher [26]

The major limitation of this testing facility [26] was the test sample scaling, impactor size and velocity restrictions and recording of the test data. Only qualitative data, such as localised damages, cracks, and penetration of the impactor, were recorded. While the quantitative data recording for deformation and crack widths measurement can be facilitated by additional measuring accessories [27-32], flexibility of changing impactor mass, velocity and scaling of samples for realistic horizontal impacts are the major challenges for the available testing facilities. In addition, studies on global response of infrastructure to credible impacts to minimise damages and potential causalities through appropriate retrofitting is important. While numerical simulations of impact events provide an effective means of examining such scenarios, without credible data, mathematical simulations based on highly nonlinear and complex theories will not be able to provide reliable outputs. Therefore, a versatile impact testing facility that can be configured for various scenarios such as size of structural samples made of different materials, changing impactor mass and velocities, braking system for impactor safety with detailed data measurement options is required for this purpose. At present, there are no lateral impact facilities available to represent realistic horizontal impact scenarios on the structures such as car collisions, blast events or debris impact for varied structural elements, impact forces and velocities.

This paper presents the details of the design and manufacture of a versatile new generation testing facility capable of experimentally simulating realistic impact scenarios involving a projectile of varied masses from 100kg to 200kg with velocities up to a maximum of 50 m/sec. This machine can simulate low velocity (such as low wind pressures, punching of anchors into walls during earthquakes, low speed car impacts with walls, etc.) to high velocity impacts (debris impact under strong winds, high speed vehicular impacts, certain blast events, etc). In addition to the impact testing machine, other sophisticated accessories for data acquisition are designed, assembled and synchronised with the operation of the equipment. The designed data acquisition system has the ability to record quantitative and qualitative results during the impact. Quantitative results are recorded from the projectile and target structure separately. Data recorded internally in the projectile include triaxial accelerometers to determine the impact force vector, from launch until impact conclusion. Similarly, data from the target structure in terms of acceleration, vibration, deformation, strain contours on the surface, and the reaction force from the supports are acquired. In comparison, the qualitative results include crack propagation and classification of the various failure modes of the target structure. The quantitative results at every 0.02 milliseconds using high speed DIC (digital image correlation) camera at 50,000 frames per second can also be recorded during penetration phenomenon at high velocity impacts. During low velocity impacts, the cracking widths on the surface or through the thickness of the target structure can be recorded at the same speed through 3D digital image correlation cameras and software. The projectile's energy dissipation due to the braking mechanism in the equipment during the impact can also be evaluated for the forensic investigation of the structure.

Section 2 presents the description of the individual mechanical and electrical components and their assembling into the impact testing machine. A subsection on the DIC technique is also introduced for data recording through two high speed cameras during testing. The cameras' configuration used to measure the strains and displacements in all three directions on the target structure using the DIC technique is discussed in detail. Earlier, this technique was used by the authors to obtain strain and displacement profiles of the specimens only in 2D [33-36]. The potential use of this impact testing machine for two different structural testing programs is discussed in section 3. This discussion includes the test frame setup and the camera setup required to optimise the space and resources available in the laboratory without compromising the data acquisition from the impact testing machine and the target structure. Section 4 summarises the main features and use of the impact testing machine.

2. Impact Testing Machine

The pneumatic impact tester stores energy in the form of compressed air in a pressured vessel which is then rapidly released to propel a cylindrical piston/projectile along a barrel towards the impact target specimen. Despite its scale, this arrangement is relatively easy and cost-effective to make. To achieve the desired maximum 50m/s projectile exit velocity, the stored air must be applied to the rear of the projectile as quickly as possible. Conventional ball and gate valves are typically too slow to achieve the required energy transfer rate. A solution is to use the projectile body as a shuttle valve. The pressure vessel is directly coupled to the rear of the barrel until the projectile is fully retracted into the rear of the breech flange and thus blocking the port to the barrel. A two-position solenoid operated 12.5mm pneumatic ball valve either safely vents to atmosphere or provides a pilot pressure to the rear of the projectile. Once pilot pressure is applied to the projectile, it slides forward through the O-ring seals for about 10 mm before uncovering the main pressure vessel port. The air flow rate will then snowball as the projectile continues to move forward until the port is completely open and the maximum rate achieved. The pressure in the pressure vessel can be varied according to the projectile mass to achieve the desired velocity and energy of the projectile before firing. Safety interlocks in the control valving and positive locking pins on the projectile prevent unintended operation.

The mechanisms involved in each component of the impact machine are explained in detail in three subsections, (a) Mechanical setup, (b) Electrical setup and (c) DIC setup for recording and analysing the results.

2.1. Mechanical Setup

This section is subdivided into two subsections, a detailed description of the individual mechanical parts and assembly of the impact testing machine. The mechanical components of the machine are (a) Pneumatic System (b) Cannon (c) Braking System (d) Projectile and (e) Base Support Frames.

2.1.1. Individual components

a) Pneumatics: Pressurised air enables the motion of the projectile in the barrel. For the projectile motion, it is important to know the exit velocity of the projectile from the cannon so that the required air pressure can be calculated. The basic theory is that the cannon is powered by gas expansion in the barrel, which causes the projectile to be flung forward by the force of the expanding gas. This mechanism illustrates various physical phenomena such as recoil, conservation of momentum, work-kinetic energy theorem and air drag. For the present impact testing facility, the compression of gases is controlled by attaching an "Air Amplifier" system connected to the pressure vessel as shown in **Figure 3**. This system can increase normal pressure of 4 bar or 6 bar to the desired final pressure up to 30 bar. Air amplifier is supplied with an air control unit comprising a filter, pressure regulator with pressure gauge and an air shut-off valve. The pressure vessel and the air amplifier for the impact testing machine are shown in **Figure 3**. The pressure vessel is controlled by a Pneumatic control system.

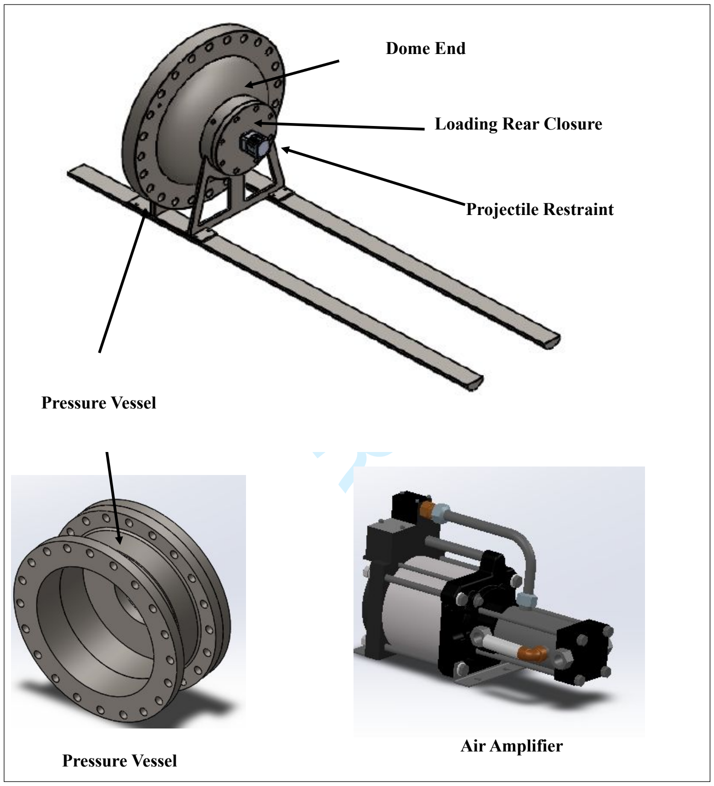

Figure 3: Pressure vessel and the air amplifier system of impact testing machine

Pneumatic control system is installed on the impact machine (as shown in **Figure 4**) to control the vessel's pressure, which helps in the projectile's motion in the barrel. The main components of the system are (a) compressor, (b) pressure gauge, (c) control valves, (d) ½" connecting tubes and fittings and (e) various 24VDC solenoid actuated ball valves and needle valves. The power requirement for the components of the control system is 240VAC 3A single phase.

Most pneumatic process control valves and fittings are designed for an upper working pressure of 10 bar. The cannon pressure vessel is intended to operate at 25 bar with an upper limit of 30 bar, so careful component selection was required for the high pressure parts of the system. The pneumatic circuit was designed as much as possible to be safe so that in the event of a power loss the default spring return positions of the valves would safely vent the pressure vessel. In addition, each of the critical ball valves required for pressurising and launch, have both visual and limit switch feedback switches to confirm their position status with the controller. Emergency Stop buttons are configured to vent the pressure vessel and disable the launch solenoid valve independent of the automatic control system.

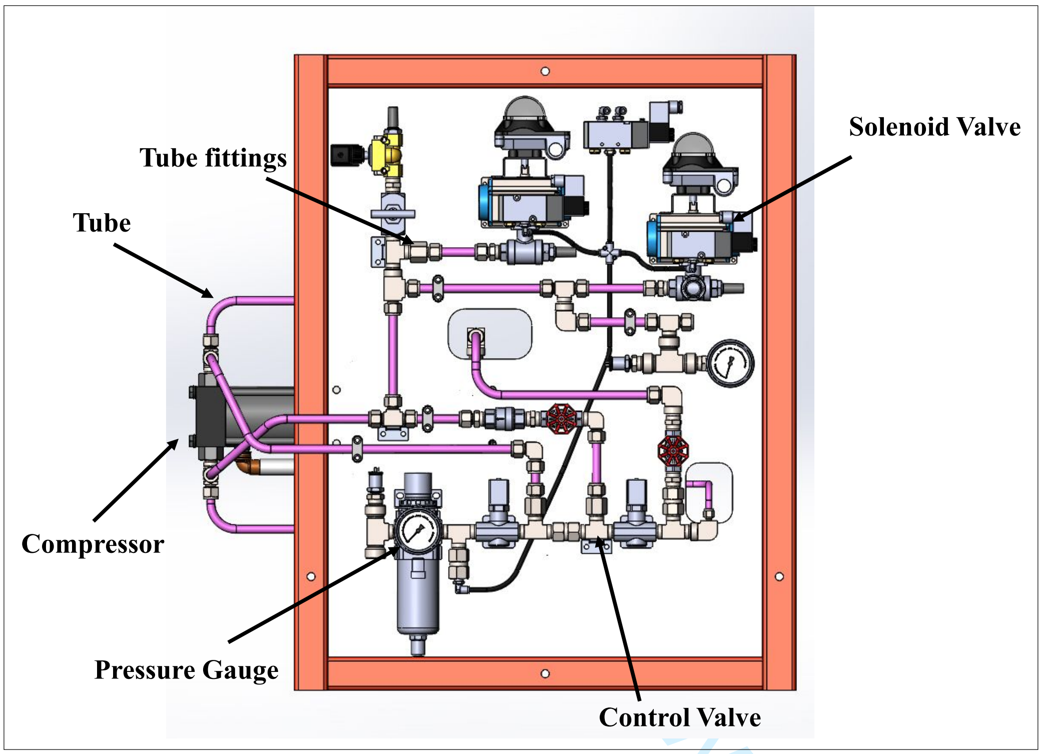

Figure 4: Pneumatic control system with control valve and other fittings

b) **Barrel:** The barrel is fabricated from a seamless precision hydraulic cylinder tube made from cold-drawn ST52 steel. The internal bore of hydraulic tube is extremely straight and round with a very smooth ground surface finish. ST52 steel grade is low carbon manganese steel with a yield strength of 542 MPa and prone to corrosion. Normally the external surfaces of hydraulic cylinders are painted, and the internals sealed from atmosphere and covered with hydraulic oil. The bore of the impact tester is fully exposed to the air and hence electroless nickel plating was used for corrosion protection and its low friction. The barrel was designed so that it could be manufactured and fitted without welding. The heat of any welding process would distort the barrel and/or damage the plating. The barrel features an array of vent slots in the centre of its length as shown in **Figures 5(a) and 5(b).** These vents exhaust the remaining air pressure from the launch to prevent it acting further on the rear of the projectile and contributing to impact energy. Thus, the projectile energy is purely a function of its mass and velocity.

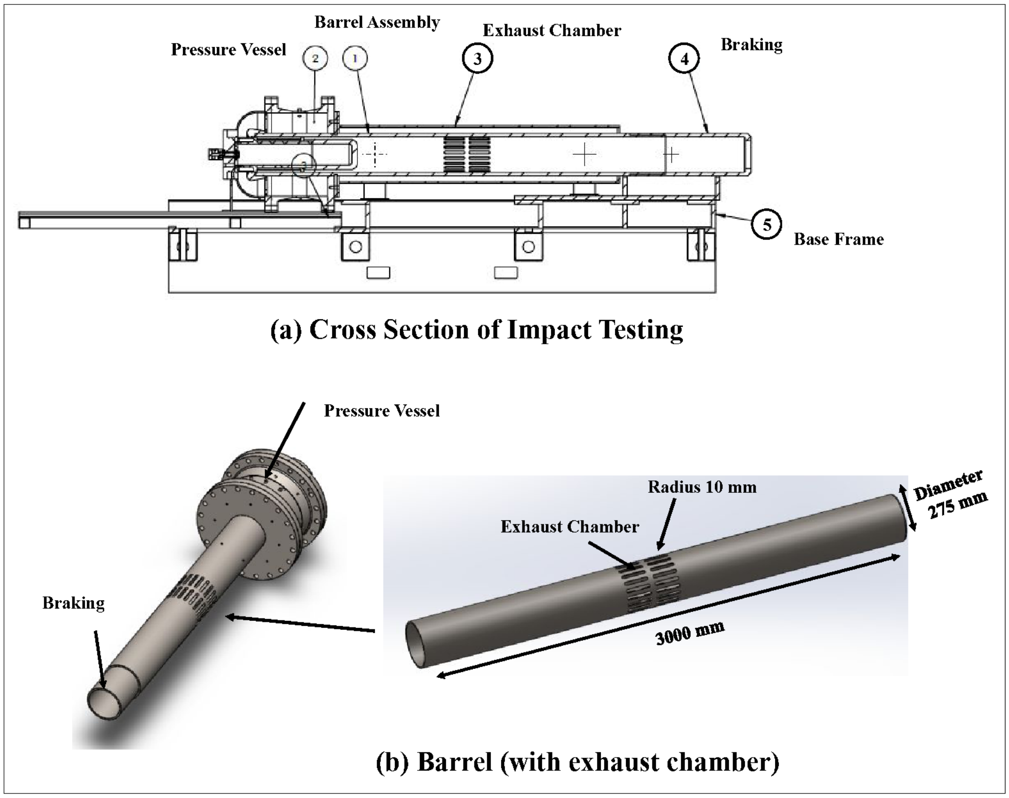

(a) Cross Section of Impact Testing

(b) Barrel (with exhaust chamber)

Figure 5: Impact testing machine components (a) cross-section of machine, (b) barrel with exhaust chamber.

Figure 6: Barrel with attached pressure vessel arriving from manufacture ready for installation and fit-out at the structural testing laboratory of QUT (Queensland University of Technology, Brisbane Australia).

Braking system: An aluminium crush tube is placed in the brake sleeve to act as a braking system for the projectile motion, as shown in **Figure 7**. The brake sleeve (shown in **Figure 7(b)**) is supported with a flange to stabilise the barrel while crushing the tube. The crush tube will only be consumed if the test specimen fails to absorb the impact. The amount of impact energy absorbed by the test sample will depend on its type and material and the impact testing speed. Ductile metals may absorb more energy which might result in nil to low crushing of this tube, whereas for brittle materials, energy might dissipate through early cracking and crush tube will then engage to absorb the impact energy and reduce the speed of projectile for safety. Impact speed will also affect the engagement and crushing of aluminium tube.

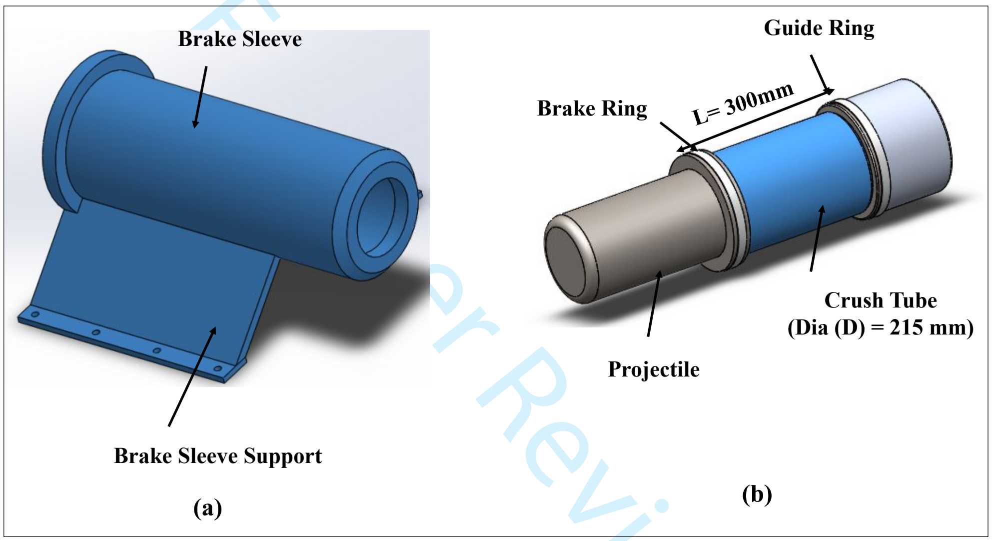

Figure 7: Braking system in the machine (a) Brake sleeve (a protective cover on the top) and (b) Crush tube attached to the projectile

Crushing test of the tube under direct compression is shown in **Figure 8.** The reason for selecting the aluminium tube for braking or absorbing energy is due to the unique failure modes of folding under compression. When a circular thin-walled tube is crushed axially, it collapses either asymmetrically or non-symmetrically, depending primarily on diameter to thickness (D/t) ratio and the length to thickness (L/t) ratio of the aluminium tube. The axisymmetric failure mode is often known as the ring mode or concertina mode, while the non-symmetrical mode is called the diamond mode. The number of lobes characterises the diamond mode. However, for certain values of D/t ratios, the tube might start to collapse with the ring mode and then switch to the diamond mode, hence exhibiting a mixed-mode crushing failure. The size of the crush tube in this projectile is 300 mm (L), 215 mm diameter (D), and the thickness (t) of the tube is only 4 mm. Hence the L/D and D/t ratios are calculated as 1.4 and 53.8, respectively. According to past research studies, if the L/D ratio and D/t ratio lie between 1 to 3 and 10 to 80, respectively, the crush/failure mode is ring or concertina mode [37, 38]. Crushing tube test results when cut into two halves (in **Figure 8 (c)**) also proved the same ring mode of failure, which is necessary to enable it to fit well in the cannon after crushing. It must be mentioned here that although the crush tubes were not tested under dynamic loading, it is evident from the literature [37,38] that the failure mode remain the same for the dynamic load as well. Each crush tube can cost up to AUD 200-300 for fabrication for this impact testing machine.

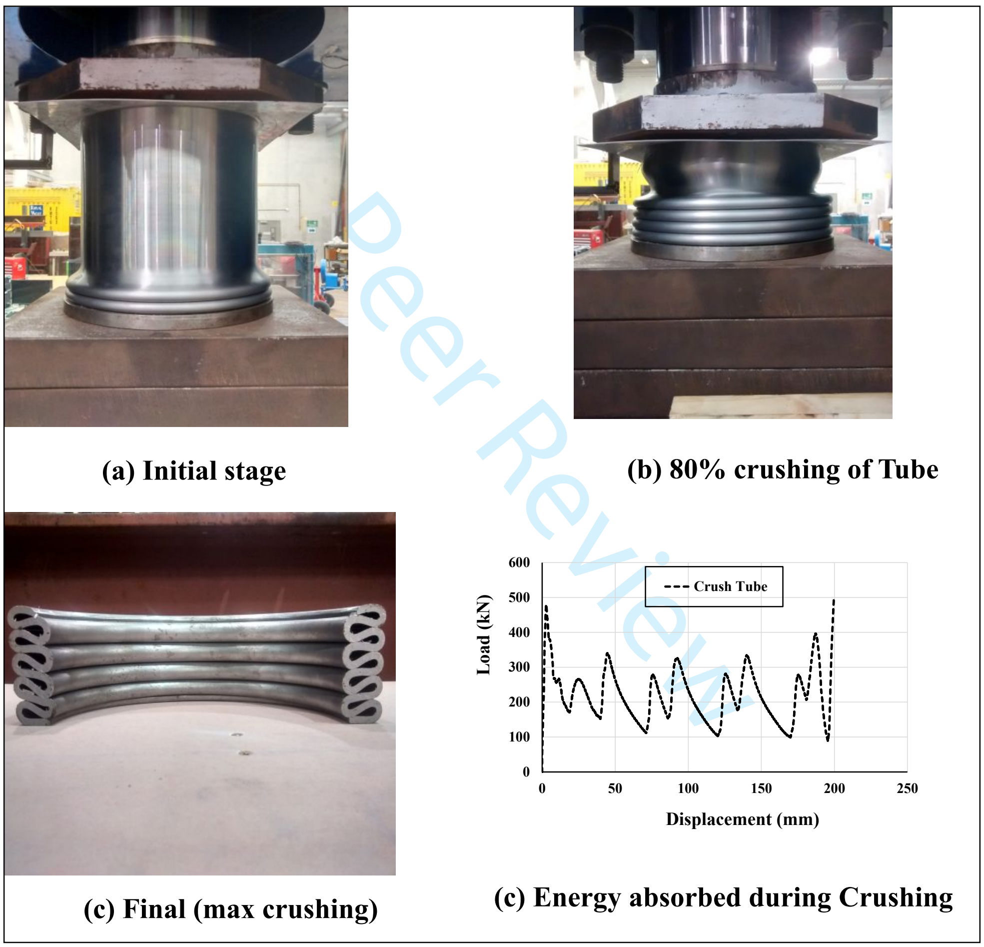

(a) Initial stage **(b) 80% crushing of Tube**

(c) Final (max crushing) **(c) Energy absorbed during Crushing**

Figure 8: The failure modes of tube crushing at different stages (a) initial stage, (b) 80% crushing of tube, (c) final stage (cross section)) and (d) load-displacement curve during crushing

c) **Projectile:** The mechanical design and manufacture of the projectile includes the encoder grooves and hardening of the nose. The material used to construct the projectile is high strength steel hardened at the nose which can resist a stress of up to 800 MPa during impact. The projectile of diameter 200 mm moves inside the barrel of 250 mm diameter. Its nose is assembled with the encoder magnetic sensor design to record the impact force when it comes in contact with the target structure. The shape of the projectile for the initial level of testing is manufactured as an elliptical nose. However, there is flexibility to change the nose shape of the projectile to a flat circular head of 200 mm diameter or a flat square head with a maximum diagonal length of 200 mm as shown in **Figure 9**.

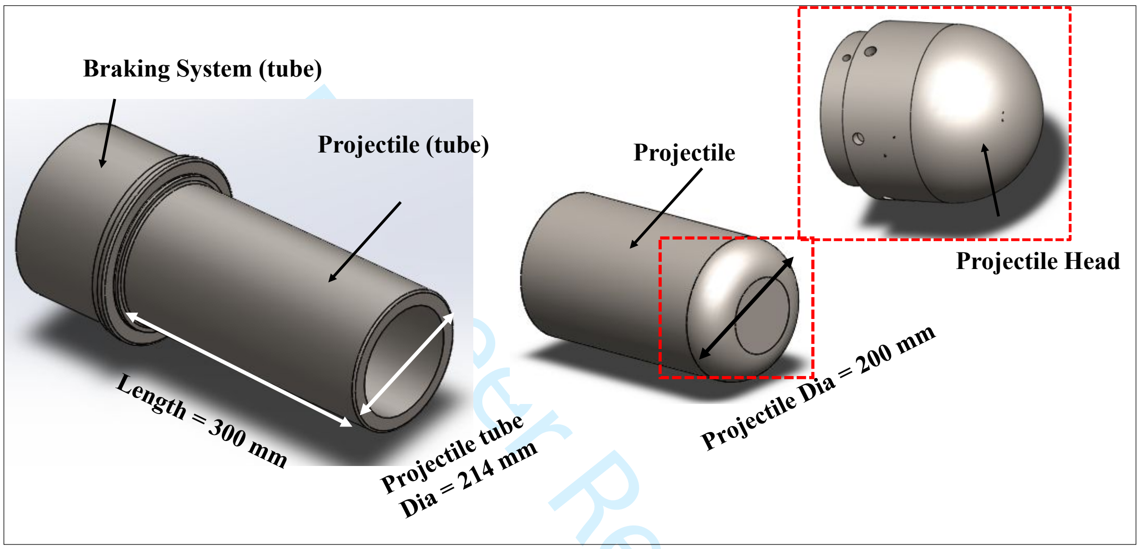

Figure 9: The projectile with elliptical nose fitted inside the impact testing machine

d) Base Support Frame: The base frame support system shown in **Figure 10** includes the "frame base" attached with the "slide frame" to support the firing and recoiling of the system when the projectile is fired at a very high velocity. The "vessel support flange" is attached to the frame base to provide extra support to the pressure vessel of the pneumatic system to remain steady at the time of firing. The barrel and attached pressure vessel require strong support due to the large amount of energy absorbed during the crushing of the tube inside the barrel. The entire system will be assembled and attached to the strong floor as shown in **Figure 11 (a)** using the strong bolts provided at the bottom of the frame. This bolting system will provide the flexibility to change the orientation of the impact tester or move it away from the strong floor when not in use. **Figure 11 (b)** shows the manufactured frame assembled in the QUT structural laboratory.

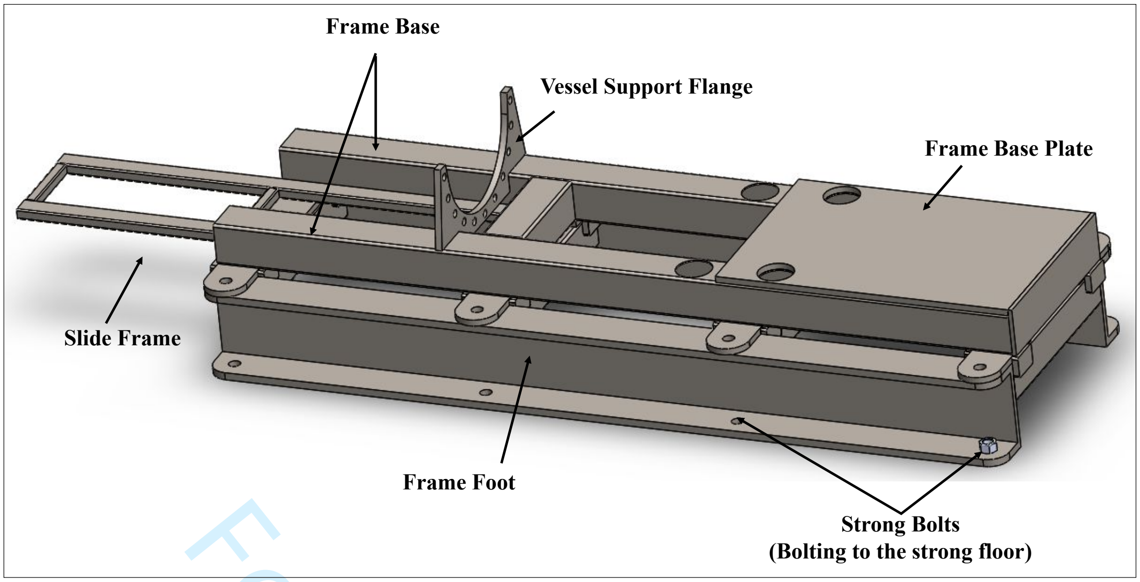

Figure 10: Frame base attached with the slide frame

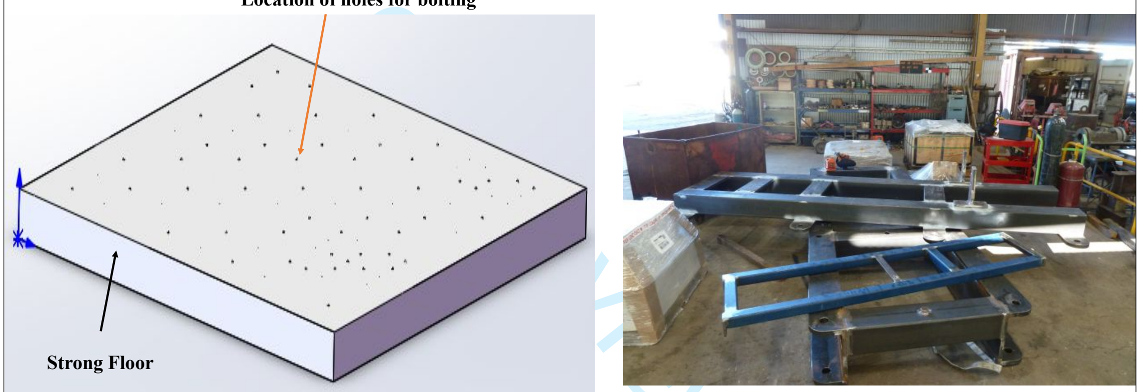

(a) Strong Floor: Impact testing Machine (b) Frame assembling in Laboratory

Figure 11: (a) Strong reinforced concrete floor and (b) frame assembled in the laboratory

2.1.2. Assembly of components

This subsection presents the assembly of all individual components described in **Section 2.1.1** for the manufacture of the impact testing machine. The overall dimensions of the impact testing machine are **6.5 m (Length) × 1.5 m (Width) × 1.5 m (Height)** after assembling the components all together, as shown in **Figure 12**. The total weight of this equipment is around 5 tonnes, which helps to provide stability to the equipment at the time of firing and recoiling. In addition, it is bolted with 40 mm high grade steel bolts to the reinforced concrete strong floor at 8 locations.

While performing tests, it is suggested to maintain a 1 m clearance on all sides of the equipment to maintain safety. Operators must also establish and enforce appropriate exclusion zone when the impact tester is in use. The pneumatic vessel is required to be filled with standard gases pressurised to 6.5 bar. During operation, the gas rushes to the vessel at a rate of 100-200 litres/min.

The impact testing machine needs to comply with the safety regulations before conducting tests. According to Australian regulations (AS 4024), a professional engineer needs to carry out critical safety checks, for example, (a) robustness of the assembly of the equipment on the strong floor, (b) firing and braking mechanisms (c) control system including the mechanical and electromagnetically operated control valves attached to the pneumatic pressure vessel, (d) robustness of the loading frame design for supporting the target structure and (e) specimen lifting jig design for the target structure. In addition to this protocol, the tester needs approval in the laboratory via detailed risk assessment and management, for preparation, testing and data recording.

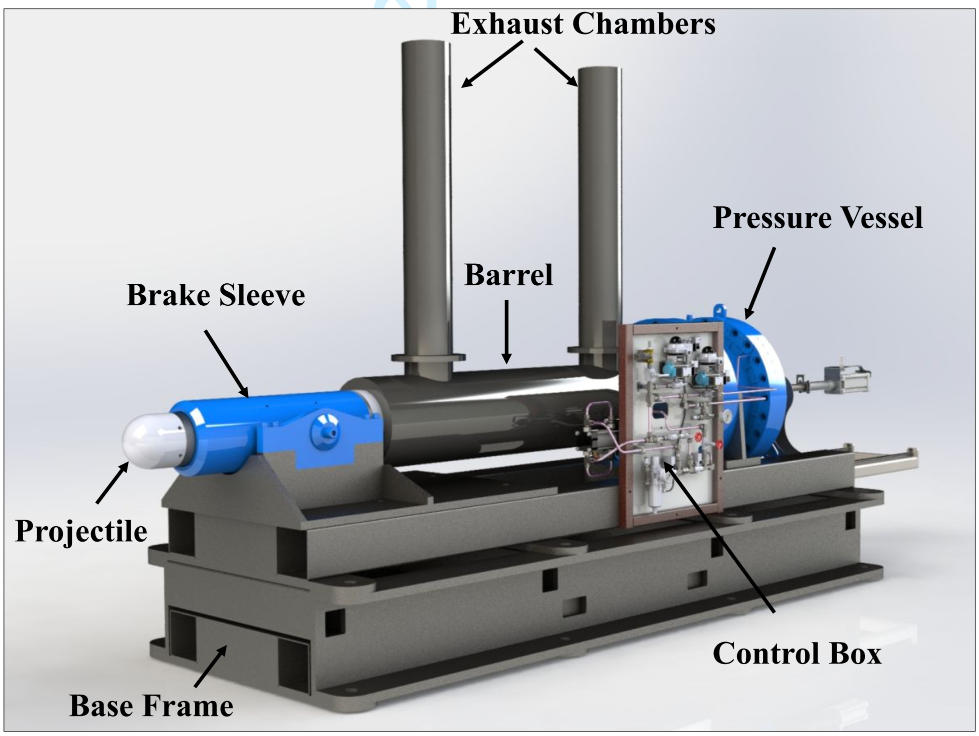

Figure 12: The impact testing machine with all individual mechanical components assembled.

2.2. Sensors and Data Acquisition System

This section presents the details of the components used for collecting impact test data. The components are (a) Projectile sensors and (b) Data acquisition system.

(a) Projectile sensors: Projectile nose encoder magnetic sensor provides high fidelity projectile position and velocity data. The details of the sensors are provided below:

(i) Accelerometers: A Piezoresistive (PR) shock accelerometers weighing only 2.83 gm are ideal for measuring long duration shocks. The sensitivity of accelerometers (± 60,000g) is 0.001V/g and can effectively work within the temperature range of -51^{0}C to 121^{0}C. These accelerometers are passive devices that require stable external power, typically a regulated dc voltage such as 10V. The output from the sensors is typically routed to a bridge conditioner then an oscilloscope or various data acquisition instruments. These full-bridge sensors include four active silicon strain-sensing elements which change resistance proportionally to an applied acceleration. During mounting PR accelerometers into a projectile, it is important to check characteristics such as location, temperature, environment, and surface condition. The battery operated DAQ system for the sensors is attached with the accelerometers inside the projectile to record the vibrations. The sensors must be mounted on a clean, flat surface to avoid the potential for misalignment and limited contact with the mounting surface, which may diminish the sensors' performance.

(ii) Strain gauges: The strain gauge selection process for this impact testing machine was according to the following requirements: (a) accuracy, (b) stability, (c) temperature, (d) elongation in the gauges, (e) cyclic endurance, (f) ease of installation and (g) compatible with the environment. The alloy used in the strain gauges is "Constantan", which has high strain sensitivity and high-temperature resistance of about 65^{0}C. Strain gauges are wrapped with an RTV (room-temperature-vulcanising) silicone rubber layer that offers water resistance and attached inside the projectile. The gauge length for the strain gauges ranging from 0.2 mm to 0.3 mm tends to integrate, or average, the strains over the area covered by the gauge length. The high resistance strain gauges of 350 Ω are used to enhance the advantage of decreasing the lead wire effects; such as circuit desensitisation due to lead wire resistance and unwanted signal variations caused by lead wire resistance changes with temperature fluctuations.

(iii) Displacement transducers: Displacement transducers or sensors consist of semiconductor lasers with a continuous wavelength of 660 nm . The series includes 25 sensors with a range of 2 mm to 1250 mm and a base distance from 15 mm to 260 mm. The sensors are intended for non-contact measuring and checking of position, displacement, dimensions, surface profile, deformation, vibration, sorting and sensing of technological objects, and measuring levels of liquid and bulk materials.

Operation of the sensors is based on the principle of optical triangulation shown in **Figure 13**. Radiation of a semiconductor laser 1 is focused by a lens 2 onto an object 6. Radiation reflected by the object is collected by a lens 3 onto a linear CMOS (metal-oxide-semiconductor or active pixel sensor) array 4. A CMOS image sensor has an amplifier for each pixel which results in the use of less power and provides fast readout when fewer components are attached to a smaller area. The signal processor 5 calculates the distance to the object from the position of the light spots on array 4.

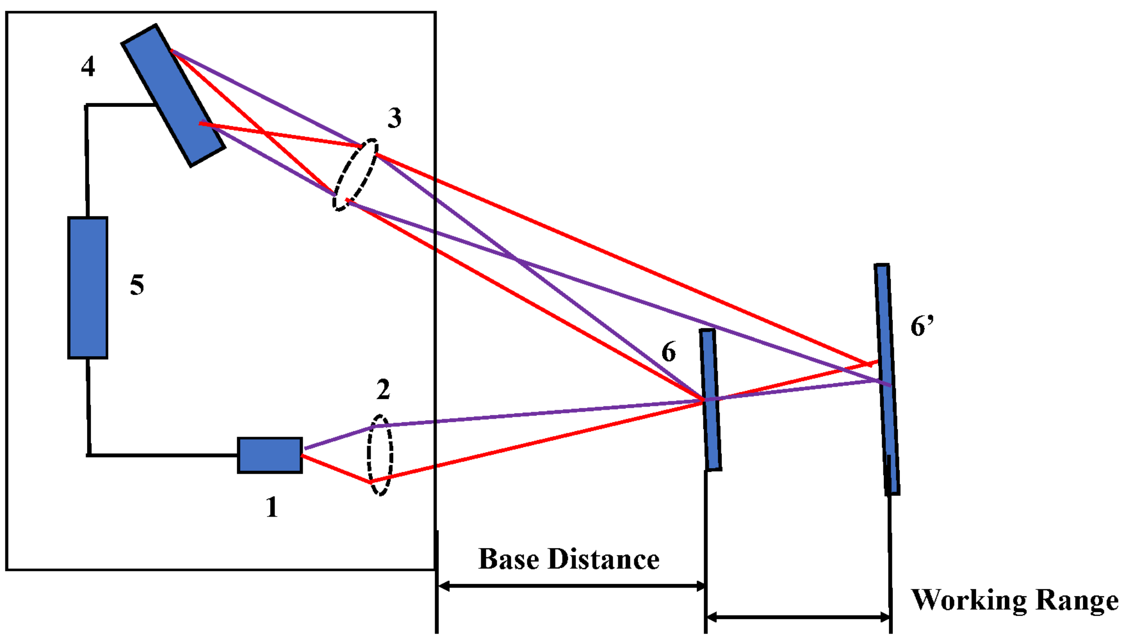

Figure 13: Principle of optical triangulation used in displacement transducers

The sensors work under a maximum frequency of 180 kHz or the integration time limit response ≤ 5μs. The parameter "time limit for integration" specifies a maximum allowable time of integration. If the radiation intensity received by the sensor is of small magnitude that no reasonable result is obtained within the time of integration, the sensor transmits a zero value.

(b) Data acquisition electronics (DAQ): A DAQ system is programmed designed, built and wired inside the projectile. This independent DAQ system can record 3 axis accelerations of up to +/- 60,000g and a 3-axis force vector of up to 4 MN. It records each channel at 250 kS/s (kilosamples per second), and the data is stored internally and recovered via a USB port at the end of the impact test. In data conversion, an analog signal is converted to a number of streams, each representing the analog signal's amplitude at a moment in time and each number is called a "sample". The number of samples per second is called sampling rate and it is measured in samples per second. A sensor panel with 32 channels of DAQ with 16-bit minimum resolution and a minimum of 250 kS/s per channel is attached to the testing machine. The inputs required will be from a mixture of strain gauges, bridges, IEPE (Integrated Electronics Pizo-Electric) accelerometers; a type of piezoelectric sensors which contain built in impedance conversion electronics, DC accelerometers and linear voltages from laser displacement transducers. The storage device is set up to provide sufficient memory to record 32 channels at maximum sampling speed and resolution for the duration of impact test. DAQ trigger attached to the system has the capability to synchronise DAQ with camera capture.

(c) Accelerometers for Target Structure: Twenty **s**ingle axial piezoelectric accelerometers are used to record the dynamic response of the target structure when subjected to the impact. The accelerometers can measure lateral and vertical accelerations depending on the orientation of the accelerometers attached to the target structure. The acceleration data is acquired by a centralised National Instruments (NI) data acquisition system which requires: (a) NI DAQ 9172 chassis, (b) NI 9234 dynamic signal acquisition modules, and (c) an in-house LabVIEW based data acquisition program to enable precise hardware-based synchronisation and data analysis [39]. The sensors incorporate the quartz element, which enhances the sensitivity of compressive and shear loads. The accelerometers will be connected to an electronic device for converting the charge signal into a voltage signal proportional to the mechanical forces. The accelerometer sensitivity is 0.15 V/g within the measuring ranging ±20,000g. The acceleration data is captured in the time domain and is conveyed to the modal analysis software to retrieve modal parameters. Natural frequencies and mode shapes are then extracted by the data-driven Stochastic Subspace Identification (SSI-DATA) in modal analysis software [40].

2.3. DIC Setup

The DIC method is used to quantify the impact damage in the target structure in terms of deformations and strains. It comprises 2 High-Speed (HS) Cameras (**Figure 14(a)**) that can record at >=50,000 fps and are mounted on tripods, designed and built specifically for capturing 3D views of the impacted specimens. A standalone frame for each HS camera and lighting (**Figure 14(b)**) are built and assembled near the impacted specimen. The other accessories attached to the setup are (a) designed and built cable breakouts for target DAQ to suit sensors, (b) customised laptop with high CPU capacity and performance, (c) 4 x LED lights and (d) lighting tripods and trusses to hold the lights. Details of the DIC components used for capturing the target structure are provided in detail below.

(d) Camera: Two HS cameras with high performance are configured with the impact testing machine to quantify the response (damage and failure) of the target structure during the impact. They have the best possible monochrome resolution with aspect H:V ratios between 1:1 and 2:1. The cameras have very high sensitivity with low noise in the data analysis when recording at the rate of 50,000 fps, equating to 1 mm maximum displacement between frames at 50 m/s projectile or target velocity. The cameras have shutter speeds that are fast enough to record <0.1 pixels of blur at 50 m/s with the best resolution @ 50,000 fps and 400 mm FOV (field of view). The digital system using the pulsed type of light sources attached with the camera can synchronise the two cameras together. The configured system can initiate an image capture sequence from a digital edge signal at launch or upon exit from the barrel. The memory storage required for at least 1 second of testing at 50,000 fps capture is calculated as shown below:

Projectile time to exit the barrel is $100\text{ms} @ 50\text{m/s}$ and total time elapsed in testing $= 1\text{sec}$

(i) Assume resolution of image recorded at 640×480

$\text{Total Pixel} = 640 \times 480 = 307200 \text{ Pixels}$

monochrome image of depth $= 8$ bits

$$\text{Total Memory} = \frac{307200 \times 8 \times 50000 \times 1}{8 \times 1024 \times 1024 \times 1024} = 14.30 \text{ GB (Gigabytes)}$$

(ii) Assume resolution of image recorded at 1280×896

$\text{Total Pixel} = 1280 \times 896 = 1146880 \text{ Pixels}$

monochrome image of depth $= 8$ bits

$$\text{Total Memory} = \frac{1146880 \times 8 \times 50000 \times 1}{8 \times 1024 \times 1024 \times 1024} = 53.4 \text{ GB (Gigabytes)}$$

These calculations show that a test recorded for 1 sec at minimum and maximum resolutions can generate the data file within a range of 15 GB to 54 GB, respectively. This information helps to define the configuration required for the laptop to store and analyse the recorded data from the sensors attached to the machine and the target structure.

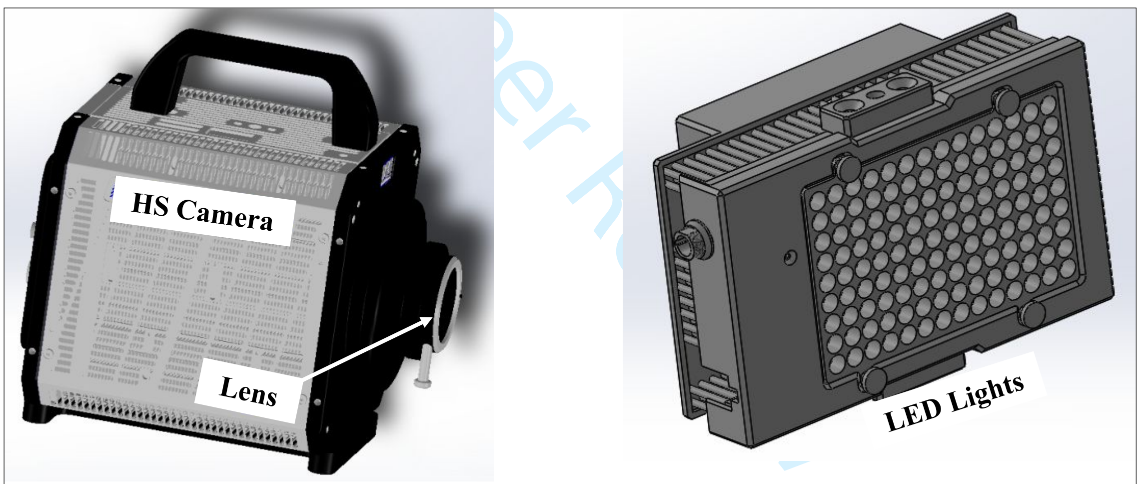

(a) High Speed Camera **(b) MultiLED Lamps**

Figure 14: Data recording system includes (a) High-speed camera (s) and (b) Multi Led lights

The positioning of the cameras is an important aspect of the entire testing programme. During the time of contact between the projectile and the target structure, the visibility of the contact area will be minimum if the camera is placed in line with the projectile motion. Hence, the camera position is reasonably calculated on the assumption that the target structure can deform from 1 mm to a maximum value of 240 mm from the centre of the contact region. Calculations based on this assumption recommend that the camera can be placed at a distance of 700 mm from the target structure oriented at an angle of 35^0 from its front face, as shown in Figure 15. Additionally, the gap between the impact machine and target structure should be kept at 100 mm, as shown in **Figure 15**. The maximum gap between the impact machine and the target structure is however limited to 300 mm from the face of the target structure.

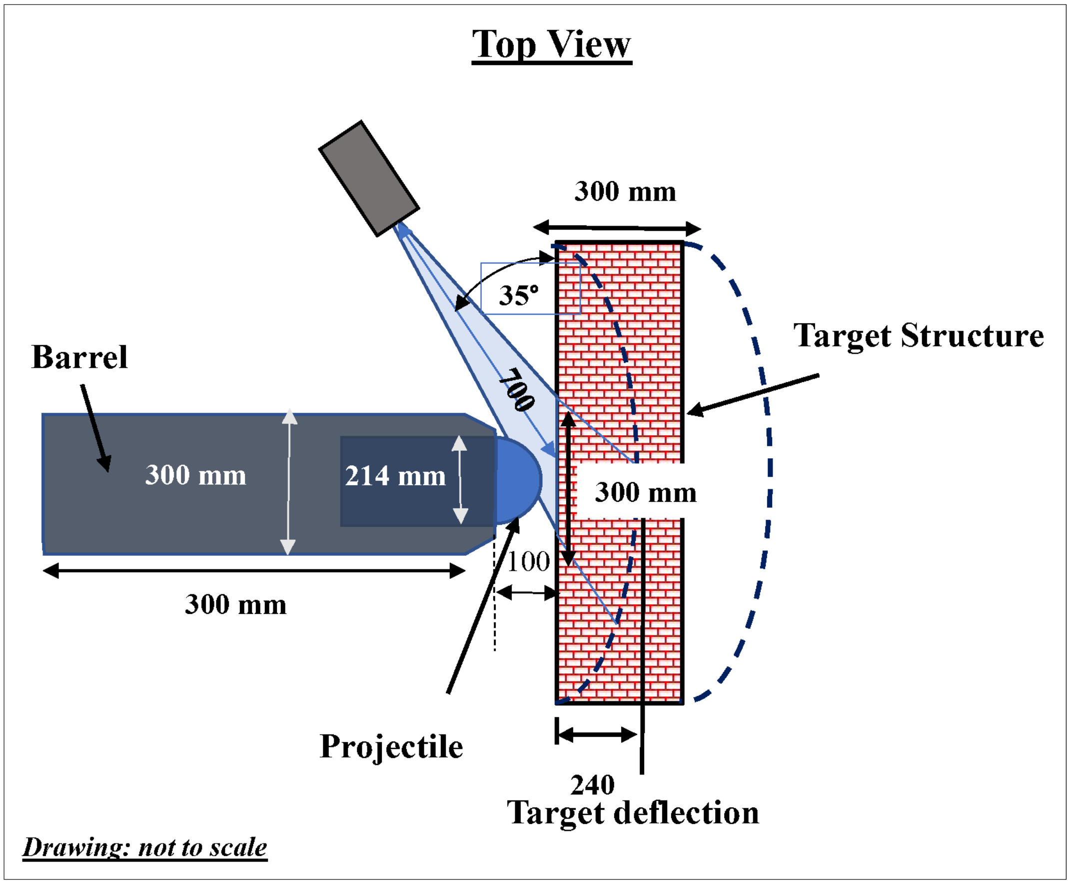

Figure 15: Orientation and positioning of a HS camera for recording data on the target structure

(e) DIC Analysis: 3D (three-dimensional) full-field, DIC analyses can measure contours, deformations, vibrations, and strains over the surface of a variety of target specimens. The system uniquely combines the high spatial resolution of full-field optical measurement with high temporal resolution. The dynamic range is from static to more than 100,000 Hz, capable of measuring displacements from micron to meter range. DIC identifies features on a surface and tracks their relative displacements frame to frame. A single-camera DIC system can only resolve purely planar (X, Y) displacements. In contrast, two or multiple camera DIC systems utilise the binocular vision principle to resolve 3D (X, Y, Z) displacements. All DIC systems utilise complex interpolation techniques to achieve about 100 times resolution than the basic camera pixel resolution in the XY plane and about 50 times in the Z-axis (depth).

For this impact machine, 3D DIC analysis relies upon two cameras to view the same region of interest (ROI) marked on the target structure. Two spotlights are positioned on either side of the cameras to achieve appropriate lightening of the ROI. Lighting positions and intensity are adjusted to achieve sufficient, uniform image contrast, comparable across both cameras when configured with a lens aperture of f16 and a camera shutter speed of 1/10,000 s. The Multi LED lamps with luminous flux of 50,000 lumens (equivalent to 500 Watt) (**Figure 14(b)**) are compatible with all applications of high-speed cameras, and they provide enough light to close the aperture at some microseconds exposure time fully. The accuracy of the processed results depends on the calibration of the images within the ROI.

The basis of the DIC calibration is to compare a known input with a measured output in terms of different defined states of measurements. Accuracy of the DIC can be established confidently based on the accuracy of the calibration. The DIC measures the change in the length to compute the strain on the surface. A non-periodic stochastic pattern referred to as a “speckle pattern” is applied on the surface marked as the region of the interest (ROI) to create an appropriate intensity field for data point creation. The camera is focused within this ROI for the deformation and other measurements. The procedure for the 3D system calibration involves moving, imaging, and analysing a rigid calibration target in front of the camera pair. The intrinsic and extrinsic parameters of cameras are calculated while the cameras’ positions are triangulated, and lens distortions are removed. This method removes any measurement bias and defines a three-dimensional coordinate system on the specimen’s surface as shown in **Figure 16.** The standard calibration target set covers fields of view from 30 mm and up. Each target usually has a matte finish and are specially coded for automatic spacing detection. These targets can be used for calibrating high-speed and low-speed systems and for both, high and low resolution cameras. The twin camera setup shown in **Figure 16** helps in setting up 3D coordinates on the surface of samples which can measure in-plane (on the surface of specimen) and out-of-plane deformation through the thickness of tested specimen.

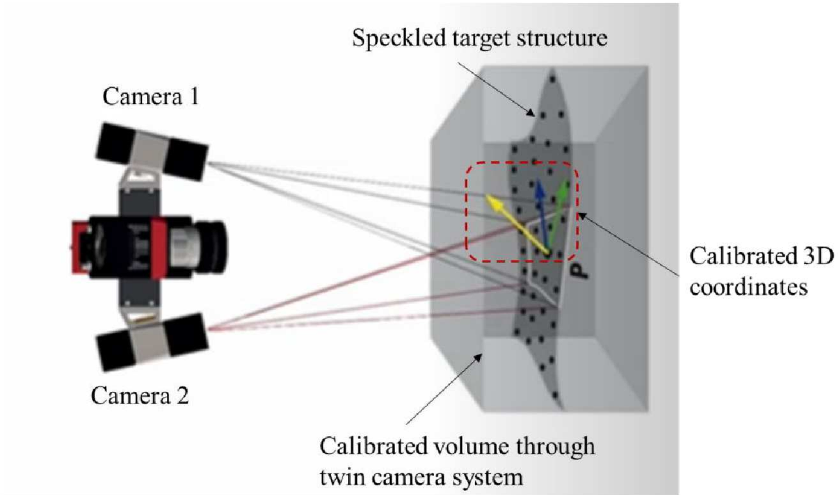

Figure 16: Twin camera DIC system and calibration

In conclusion, the mechanical components described earlier, sensors and DIC setup are essential for performing impact testing and recording substantial data for analysis. The mechanical section provides complete control on the required projectile motion and intensity for testing, while the many sensors and DIC setup enable to record sufficient data not only to perform the qualitative analysis but also to improve the quantitative measurements of the failure modes of the structural components during impact testing.

3. Potential Applications of the Impact Testing Machine

Impact testing reveals the performance of the structure under dynamic loading, for example, vehicular crashes with buildings or piers of bridges, debris impacts on buildings during tornadoes, and rockfalls during landslides etc. The potential use of horizontal impact testing can be seen in **Figure 17** which shows (a) impact of a masonry (or concrete) wall and (b) lateral impact of a concrete-filled double skin steel tube. To the best of the authors' knowledge, this innovative impact testing machine is the only one of its kind in Australia to carry out realistic lateral impact related research. Information from the testing will help to understand the impact behaviour of the target structure and to develop strategies to mitigate the adverse effects of the impact. The very first testing with this machine will be to simulate vehicular crashes onto bare and rendered masonry walls, similar to that shown in **Figure 17(a)** and to capture the effect of mitigation strategies. The strategies that will be used are quite different from traditional strategies of strengthening, as they will use high energy absorbing auxetic composite render and innovative vibration isolation at the edges of the structure [11, 20]. Subsequent testing of the retrofitted masonry walls will enable to capture the effectiveness of the mitigation strategies as well as provide valuable information for validating numerical models for use in further research.

Similarly, lateral impact testing of concrete filled steel tubes is in another research area. Using a smaller impact testing machine (previously developed at QUT), Aghdamy et al. [41] observed that CFDST (Concrete filled double skin tube) columns undergo both global and local buckling under lateral impacts. Physical inspection of the columns after impact showed that the integrity of concrete was reasonably good due to the effective confinement provided by outer and inner steel tubes. It was also found that axial load and impact location notably affect the response of the CFDST columns. The present machine which is more versatile will be helpful in future research to evaluate the performance of retrofitted CFDST columns or columns with different infill materials in/within the steel tube/tubes.

Due to the size limitation of the machine's projectile, the scaling of the samples must be carefully considered especially for walls. Half scaled wall samples can be tested for realistic impact behaviour to simulate car crashes. However, as columns have smaller cross-sectional areas, full scale columns in lateral position can be tested using this machine as shown in Figure 17(b) under axial loads of up to 400kN (in a previous project using a smaller impact testing machine). Also, end restraints can be designed specifically to account for axial shortening caused by the lateral impact force on the samples.

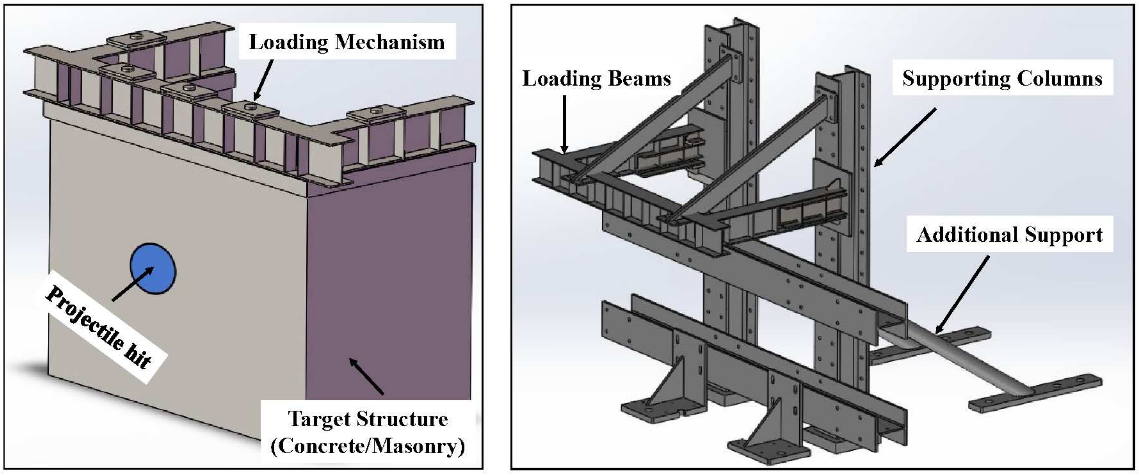

(a) Target Structure (Walls) under impact

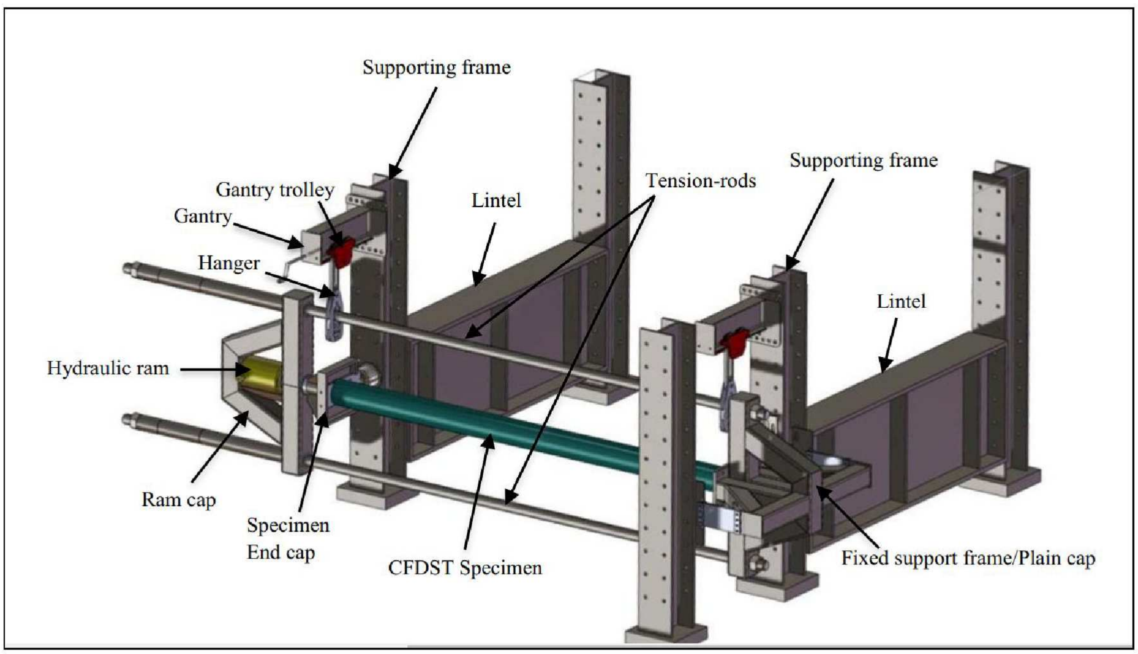

(b) Concrete filled column under impact

Figure 17: Potential impact testing: (a) masonry wall with supporting frames and (b) concrete-filled double skin steel tube with appropriate support assembly (after Aghdamy et al. [41])

Experimental testing with the impact testing machine has to be followed by post-processing of the target structure, before testing the next specimen. This process will require (depending on the amount of test data acquired), 1-3 days to remove the damaged target, process the recorded data from accelerometers, strain gauges, LVDTs etc., and perform the forensic investigation to evaluate the damage to the projectile and its sacrificial crush tube brake. If the tube is crushed, then the brake section of the impact tester has to be removed using an overhead crane and various jigs. The projectile will also be removed and dis-assembled to replace the crush tube within that assembly. After testing the internal electronics, the projectile can then be reloaded into the barrel of the impact tester using a crane or forklift with slings. The next testing can then commence, but the support structure and instrumentation may need altering to suit the test requirements. Failed or broken specimens, sometimes with fragments/small particles and dust over a large area, need proper cleaning and disposal prior to the next testing.

4. Summary & Conclusion

The development of the world-first high velocity lateral impact testing facility, which will be the only one of its kind in Australia was briefly presented in this paper. The primary emphasis was on the design and assembly of the impact testing machine, and data acquisition from the projectile fitted inside the machine and from the target structure. The impact testing machine is set up with a fully automatic firing, stopping and reloading system. Technical details of the impact testing machine and the data collected during testing are summarised in **Table 1**. The data acquisition for the target structure is managed sophistically to enhance the accuracy of quantifying the dynamic load (impact) on the target structure. The data acquisition for target structure constituent the combined use of HS cameras, Multi LED lights, strain gauges, accelerometers and LVDTs attached to the specimen. The DIC analysis creates a data size range from 14 GB to 55 GB for one specimen for the testing duration of 1 sec. The memory size of the file can vary because of the camera resolution used to record at a speed of 50,000 fps. However, for acceleration or vibration recording on the target structure will use accelerometers of ± 20,000g. Strain gauges are attached within the ROI away from the impact location to directly obtain the strains or deformation on the surface. The obtained results can be used in conjunction of the results obtained from the camera using the DIC technique. A wealth of information can be generated from testing with this machine, and this will be very valuable for (i) understanding the impact behaviour of the target structure and (ii) validating numerical models for further research. It is hoped that the new knowledge gained through research using this machine will enable effective mitigation strategies that will save lives and property during impact events.

Table 1: Summary of the impact testing machine.

Impact testing machine capacity	
Projectile Mass	100 – 200 kg
Air Pressure	3.0 MPa
Pneumatic force on projectile (& reaction force at launch)	147 kN
Acceleration	150g
Maximum velocity	50 m/s
Maximum Kinetic energy (due to a combination of mass and velocity)	125 kJ
Projectile free extension from a barrel	340 mm
Braking distance	236 mm
Projectile Max extension after braking	576 mm
Peak braking force	1 MN
Average braking force	500 kN
Braking energy	118 kJ
Mounting to a strong floor	8 bolts @ 75 kN clamp, 50 kN shear

5. Declaration of competing Interest

The authors declare that they have no known competing financial interests or personal relationships that could have influenced the work reported in this paper

6. Acknowledgements

The authors acknowledge the Australian Research Council (ARC) for the financial support to this project (under the LIEF Project). They also acknowledge the cash and in-kind contributions from QUT and the 10 partner universities. The conceptual design and the potential application of the impact testing machine was initially suggested by Manicka Dhanasekar, former Professor of Infrastructure Engineering at QUT. The authors acknowledge the original QUT

CIs: Professor David P Thambiratnam, Professor Manicka Dhanasekar (formerly from QUT), Professor Tommy HT Chan, Dr Sabrina Fawzia and Dr Xuemei Liu (now at University of Melbourne) whose time and effort enabled to win this LIEF grant. This impact testing machine was designed and is now being fabricated by the QUT technologists, Mark Hayne, and Tony Morris. The authors wish to thank them for their contribution and their continued commitment to the project.

The raw/processed data required to reproduce these findings cannot be shared at this time as the data also forms part of an ongoing study.

7. References

[1] Coleman L. Frequency of man-made disasters in the 20th century. Journal of Contingencies and Crisis Management. 2006;14:3-11.

[2] Stewart MG. Acceptable risk criteria for infrastructure protection. International Journal of Protective Structures. 2010;1:23-40.

[3] Janssens V, O'Dwyer D, Chryssanthopoulos M. Building Failure Consequences Robustness of Structures. Proceedings of the Final Conference of COST Action TU06012011.

[4] Re S. Natural catastrophes and man-made disasters in 2017: A year of record-breaking losses. sigma. 2018;1:2018.

[5] Felice GD, Giannini R. Out-of-plane seismic resistance of masonry walls. Journal of earthquake engineering. 2001;5:253-71.

[6] Freidenberg A, Aviram A, Stewart L, Whisler D, Kim H, Hegemier G. Demonstration of tailored impact to achieve blast-like loading. International Journal of Impact Engineering. 2014;71:97-105.

[7] Gilbert M, Hobbs B, Molyneaux T. The performance of unreinforced masonry walls subjected to low-velocity impacts: experiments. International Journal of Impact Engineering. 2002;27:231-51.

[8] Mauro A, de Felice G, DeJong MJ. The relative dynamic resilience of masonry collapse mechanisms. Engineering Structures. 2015;85:182-94.

[9] Topac OT, Gozluklu B, Gurses E, Coker D. Experimental and computational study of the damage process in CFRP composite beams under low-velocity impact. Composites Part A: Applied Science and Manufacturing. 2017;92:167-82.

[10] Asad M, Dhanasekar M, Zahra T, Thambiratnam D. Failure analysis of masonry walls subjected to low velocity impacts. Engineering Failure Analysis. 2020:104706.

[11] Asad M. Failure analysis and mitigating strategies for masonry walls subject to vehicular impacts: Queensland University of Technology, 2020.

[12] Maalej M, Lin V, Nguyen MP, Quek S. Engineered cementitious composites for effective strengthening of unreinforced masonry walls. Engineering Structures. 2010;32:2432-9.

[13] Ong K, Basheerkhan M, Paramasivam P. Resistance of fibre concrete slabs to low velocity projectile impact. Cement and Concrete Composites. 1999;21:391-401.

[14] Rao HS, Ghorpade VG, Ramana N, Gnaneswar K. Response of SIFCON two-way slabs under impact loading. International Journal of Impact Engineering. 2010;37:452-8.

[15] Banthia N, Mindess S, Bentur A, Pigeon M. Impact testing of concrete using a drop-weight impact machine. Experimental Mechanics. 1989;29:63-9.

[16] Cheng L, McComb AM. Unreinforced concrete masonry walls strengthened with CFRP sheets and strips under pendulum impact. Journal of Composites for Construction. 2010;14:775-83.
[17] Schmidt ME, Cheng L. Impact response of externally strengthened unreinforced masonry walls using CFRP. Journal of Composites for Construction. 2009;13:252-61.
[18] El-Salakawy E, Masmoudi R, Benmokrane B, Brière F, Desgagné G. Pendulum impacts into concrete bridge barriers reinforced with glass fibre reinforced polymer composite bars. Canadian Journal of Civil Engineering. 2004;31:539-52.
[19] Gabauer DJ, Kusano KD, Marzougui D, Opiela K, Hargrave M, Gabler HC. Pendulum testing as a means of assessing the crash performance of longitudinal barrier with minor damage. International Journal of Impact Engineering. 2010;37:1121-37.
[20] Asad M, Zahra T, Thambiratnam DP, Chan TH, Zhuge Y. Assessing vibration induced damage in unreinforced masonry walls subject to vehicular impact–A numerical study. Engineering Structures. 2021;245:112843.
[21] Asad M, Zahra T, Thambiratnam D. Failure of Masonry Walls under High Velocity Impact – A Numerical Study. Engineering Structures. 2021.
[22] Zhang J, Maalej M, Quek S, Teo Y. Drop weight impact on hybrid-fiber ECC blast/shelter panels. Proceedings of third international conference on construction materials: performance, innovation and structural applications, Vancouver, Canada2005.
[23] Kiesling E, Goolsby DEJCE. In-home shelters from extreme winds. 1974;44:105-7.
[24] Nevins NB. Experimental basis for tornado-generated missile impact resistance criteria 1993.
[25] Thompson RG. A preliminary study in missile penetration of residential walls: Texas Tech University, 1973.
[26] White BL. Impact resistance of concrete masonry walls to tornado-generated missiles: Master Thesis, Texas Tech University, United States 1986.
[27] Burnett S, Gilbert M, Molyneaux T, Tyas A, Hobbs B, Beattie GJM, et al. The response of masonry joints to dynamic tensile loading. 2007;40:517-27.
[28] Rafsanjani SH. High strain rate constitutive modeling forhistorical structures subjected to blast loading 2015.
[29] Rafsanjani SH, Lourenço PB, Peixinho N. Implementation and validation of a strain rate dependent anisotropic continuum model for masonry. International Journal of Mechanical Sciences. 2015;104:24-43.
[30] Hao H, Tarasov B. Experimental study of dynamic material properties of clay brick and mortar at different strain rates. Australian Journal of Structural Engineering. 2008;8:117-32.
[31] Acharya S, Mondal D, Ghosh K, Mukhopadhyay AKJMRE. Mechanical behaviour of glass fibre reinforced composite at varying strain rates. 2017;4:035303.
[32] Kader MA, Hazell PJ, Islam MA, Ahmed S, Hossain MM, Escobedo JP, et al. Strain-rate dependency and impact dynamics of closed-cell aluminium foams. Materials Science and Engineering: A. 2021;818:141379.
[33] Asad M, Dhanasekar M, Zahra T, Thambiratnam D. Characterisation of polymer cement mortar composites containing carbon fibre or auxetic fabric overlays and inserts under flexure. Construction and Building Materials. 2019;224:863-79.
[34] Zahra T, Dhanasekar M. Characterisation of cementitious polymer mortar–Auxetic foam composites. Construction and Building Materials. 2017;147:143-59.
[35] Zahra T, Thamboo J, Asad M. Compressive strength and deformation characteristics of concrete block masonry made with different mortars, blocks and mortar beddings types. Journal of Building Engineering. 2021;38:102213.

[36] Zahra T, Dhanasekar M. Characterisation and strategies for mitigation of the contact surface unevenness in dry-stack masonry. Construction and Building Materials. 2018;169:612-28.
[37] Guillow SR, Lu G, Grzebieta RH. Quasi-static axial compression of thin-walled circular aluminium tubes. International Journal of Mechanical Sciences. 2001;43:2103-23.
[38] Al Galib D, Limam A. Experimental and numerical investigation of static and dynamic axial crushing of circular aluminum tubes. Thin-Walled Structures. 2004;42:1103-37.
[39] Nguyen A, Chan T, Thambiratnam D, Kodikara KATL, Le NT, Jamali S. Output-only modal testing and monitoring of civil engineering structures: Instrumentation and test management. Proceedings of the 8th International Conference on Structural Health Monitoring of Intelligent Infrastructure 2017: International Society for Structural Health Monitoring of Intelligent …; 2017. p. 1134-45.
[40] Nguyen T, Chan T, Thambiratnam D. Effects of wireless sensor network uncertainties on output-only modal analysis employing merged data of multiple tests. Advances in Structural Engineering. 2014;17:319-29.

[41] Aghdamy S, Thambiratnam DP, Dhanasekar M. Experimental investigation on lateral impact response of concrete-filled double-skin tube columns using horizontal-impact-testing system. Experimental Mechanics. 2016; 56: 1133-1153